Available online at www.sciencedirect.com
ScienceDirect
Communications in Nonlinear Science and Numerical Simulation 14 (2009) 529–542
Communications in Nonlinear Science and Numerical Simulation
www.elsevier.com/locate/cnsns

Computation of the solutions of the Fokker–Planck equation for one and two DOF systems

F. Schmidt *, C.-H. Lamarque

Laboratoire GéoMatériaux, Ecole Nationale Des Travaux Publics de l'Etat, Vaulx-en-Velin, France

Received 14 May 2007; received in revised form 7 September 2007; accepted 9 September 2007
Available online 21 September 2007

Abstract

Uncertainty in structures may come from unknowns in the modelisation and in the properties of the materials, from variability with time, external noise, etc. This leads to uncertainty in the dynamic response. Moreover, the consequences are issues in safety, reliability, efficiency, etc. of the structure. So an issue is the gain of information on the response of the system taking into account the uncertainties [Mace BR, Worden K, Manson G. Uncertainty in structural dynamics. J Sound Vib 2005;288(3):423–9].

If the forcing or the uncertainty can be modelled through a white noise, the Fokker–Planck (or Kolmogorov forward) equation exists. It is a partial differential linear equation with unknown $p(X,t)$, where $p(X,t)$ is the probability density function of the state X at time t.

In this article, we solve this equation using the finite differences method, for one and two DOF systems. The numerical solutions obtained are proved to be nearly correct.

PACS: 05.10.Gg; 05.10.−a; 05.45.Xt

Keywords: Discrete nonlinear mechanical systems; Fokker–Planck equation; Energy pumping

1. Introduction

Today there is growing concern about uncertainties in dynamic structures. In fact, these uncertainties may come from unknowns in the properties of the structure or in the sollicitations, and this leads to uncertainties in the response. There exists two kinds of techniques to solve this problem: the possibilistic [6,23,1,18,17,14] and the probabilistic approaches [24,22].

The first ones just use an assessment of the interval of variation of the fluctuating parameters, sollicitations, etc. The second ones also assume a probability density function for the properties that are uncertain.

An other possibility may be the existence of an uncertainty whose origin, and thus their variations, are unknown.

* Corresponding author.
E-mail addresses: schmidt@entpe.fr (F. Schmidt), lamarque@entpe.fr (C.-H. Lamarque).

1007-5704/$ - see front matter © 2007 Elsevier B.V. All rights reserved.
doi:10.1016/j.cnsns.2007.09.004

Here we study the Fokker–Planck equation of some dynamical systems, which is a partial differential equation with unknown $p(X,t)$, where $p(X,t)$ is the probability of the state X at time t. For this, these systems are assumed to undergo a white noise, which can represent random forces or parameters.

In Section 2 we apply the theory of the Fokker–Planck equation to one-degree-of-freedom systems. We propose a simulation whose accuracy is checked. Afterwards we try to meet some deterministic phenomenons in this probabilistic study. In Section 3, we deal with a two-degree-of-freedom system leading to energy pumping. Finally, in a last part we will conclude by displaying the pros and the cons of this method.

2. Computation for 1 DOF systems

An analytical solution of the Fokker–Planck equation is known only in some specific cases, see e.g. [21,26,11]. That's why to solve the Fokker–Planck equation of the dynamical systems we study, we chose the method of finite differences, coupled with the time-splitting method [19,29,31].

Let us consider the equation of a non-linear oscillator:

$$\begin{aligned} &\dot{y}_1 = y_2, \\ &\dot{y}_2 + g(y_1, y_2, t) = f(t), \end{aligned} \tag{1}$$

$f(t)$ is a random gaussian white noise such as

$$\langle f(t)\rangle = 0, \quad \langle f(t_1)f(t_2)\rangle = \frac{W_0}{2}\delta(t_1 - t_2).$$

This noise can stand for the forcing the system undergoes, but also for uncertainties.

The Fokker–Planck equation of this system is given by [21]:

$$\frac{W_0}{4}\frac{\partial^2 p}{\partial y_2^2} - \frac{\partial}{\partial y_1}(y_2 p) + \frac{\partial}{\partial y_2}\{g(y_1, y_2)p\} = \frac{\partial p}{\partial t}. \tag{2}$$

We split the operator in three parts:

$$\frac{\partial p}{\partial t} = \mathscr{L}^* p = \mathscr{L}_1 p + \mathscr{L}_2 p + \mathscr{L}_3 p \tag{3}$$

$$\text{with} \begin{cases} \mathscr{L}_1 p = \frac{\partial}{\partial y_1}[-y_2 p], \\ \mathscr{L}_2 p = \frac{\partial}{\partial y_2}[g(y_1, y_2)p], \\ \mathscr{L}_3 p = \frac{\partial^2}{\partial y_2^2}\left[\frac{W_0}{4}p\right]. \end{cases} \tag{4}$$

So in the general case, the algorithm can be written

$$\begin{cases} p^{n+1/3} = \mathscr{U}_1(p^n), \\ p^{n+2/3} = \mathscr{U}_2(p^{n+1/3}), \\ p^{n+1} = \mathscr{U}_3(p^{n+2/3}), \end{cases} \tag{5}$$

where $\mathscr{U}_1$, $\mathscr{U}_2$, $\mathscr{U}_3$ are finite difference schemes discretizing respectively $\mathscr{L}_1$, $\mathscr{L}_2$, $\mathscr{L}_3$. They may be implicit Euler, explicit Euler, Cranck–Nicholson, etc., see next section. $p^n, p^{n+1/3}, \ldots$ are vectors of discretized states at points of the finite difference grid at discrete times $t_n, t_{n+1/3}, \ldots$ respectively.

2.1. Test of different numerical schemes and comparison with the exact solution

An analytical solution of Eq. (2) for a Duffing-type oscillator ($g(y_1, y_2) = ay_2 + by_1 + cy_1^3$) is known if and only if the non-linearity coefficient is null ($c = 0$). This solution can be found for example in [21]. We use this case to test the accuracy of our numerical solution.

We set the numerical values of the parameters according to [30]: $N = 40$, $L_1 = L_2 = 4$, $a = 2.1$, $k = 1$ et $W_0 = 3.2$, where $2N + 1$ is the number of nodes per direction, L_1 and L_2 are the length of the domain of study

in each direction. The initial condition for the algorithm is the exact solution at time $t = 0.95$ s coming from $(x_0, y_0) = (0, 0)$.

First we compare the errors of different schemes. For this, we use two representations of the error: $\|e\|_1 = \sqrt{\frac{1}{(2N+1)(2N+1)}\sum_{i,j}(p_{i,j}^{\text{exact}} - p_{i,j}^{\text{num}})^2}$ and $\|e\|_2 = \left(\frac{\sum_{i,j}(p_{i,j}^{\text{exact}} - p_{i,j}^{\text{num}})^2}{\sum_{i,j}(p_{i,j}^{\text{exact}})^2}\right)^{1/2}$.

We tried purely implicit schemes, upwind differencing, explicit, staggered leapfrog and Cranck–Nicholson.

By comparing the errors after 310 time-steps ($t = 0.973896$ s), it can be seen that in every case, a good choice may be the implicit Euler scheme because it is always stable and its error is small. On graph 1, the errors of the numerical solution obtained with different combinations of schemes are drawn:

Moreover, the calculation times of all these combinations are similar.

We also check the accuracy of the solution obtained by splitting the operator only in two parts (so with just one intermediate time-step), as in [29,31]. If we compare this way of programming with the combination of three schemes "implicit + implicit + implicit", the simulation which splits the operator with two intermediate time-steps is much more accurate and faster.

Finally, we also checked the case where the conditions at the limits of the domain of study are not null, but equal to ϵ, with $\epsilon \ll 1$. The best results are obtained with ϵ small. In fact, they would be obtained with limit conditions equal to the exact solution at the limits of the domain of study. So, for a domain of study sufficiently vast to contain all the phenomenons of the motion, null limit conditions are the best choice.

2.2. Test of different numerical values of the parameters and comparison with the exact solution

According to what has been said just before, we now use only purely implicit schemes.

While comparing the exact solution with our numerical result, we see that the error increases quite quickly until $t = \frac{\pi}{5} = 0.6283$ s (see Fig. 2). The maximum which is reached is $\|e\|_1 = 0.00051180$ and $\|e\|_2 = 0.006057$. After that, the norms of the errors decrease slowly. The time of calculation (CPU) is 4.8484375×10^2 until $t = \frac{6\pi}{5}$.

The maximum of error occurs at the states where the peak of the probability density function is located. This means that his location and his base are correct, but his height is slightly smaller in the numerical solution. But this loss of height is acceptable: between 2% and 10%. This decrease in the height of the peak is due to losses of energy in the domain of study, outside the peak, where the density of probability calculated numerically is gently bigger than it should. As the integral of the density of probability all over the domain of study is normed to 1, this makes the peak be less tall.

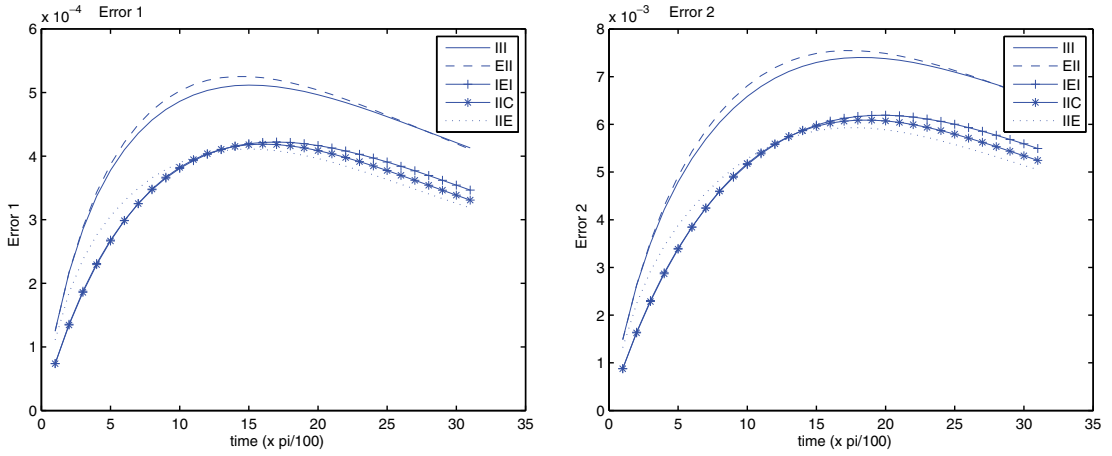

Fig. 1. Norms 1 and 2 of the error for different combinations of schemes. "I" stands for "implicit", "E" for "explicit", "C" for "Cranck–Niholson". So "III" means the combination of schemes "implicit + implicit + implicit".

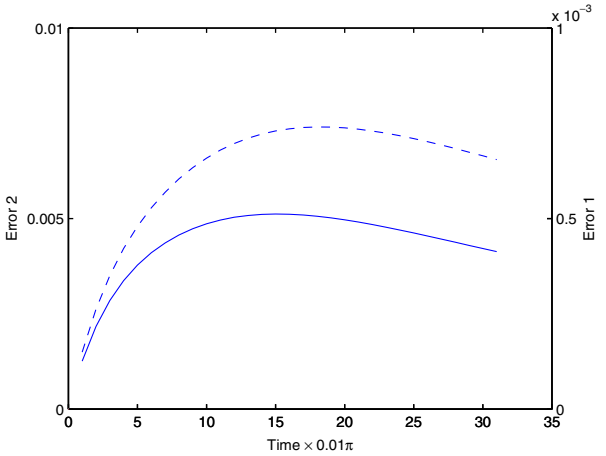

Fig. 2. Evolution of the norms of the error along time. The dotted line represents error 2, whereas the full one stands for error 1.

We now test different other numerical values for the parameters. Then we compare the numerical solution with the exact one, that is to say the analytical one.

We give the errors at $t = \frac{31\pi}{100}$ s = 0.973896 s (see Table 1):

This can be commented pertinently:

- The simulations with a too small diffusion coefficient or a too limited domain of study are unacceptable. In the first case, the reason is that because of the value of W_0, the matrix given by the Euler implicit scheme may be ill-conditioned. Then, because of the density of probability compelled to be null at the limits of the domain of study, this last one must be sufficiently large to contain all the dynamical phenomenons of the system.
- Otherwise the errors are very small. Moreover, the numerical values of the parameters chosen in [29,31] give the best result: this is the case because they may have been chosen in order to work with the best conditioned system.

To conclude this section, we claim that our numerical scheme gives good results. But a previous deterministic calculation may be usefull, in order to determinate the best domain of study (just large enough) and the best parameters for the simulation (time step, space steps, etc.) in order to work with the best-conditioned matrices.

Table 1
Norms of the error while changing numerical values of the parameters

Numerical value of the parameters	Norm 1	Norm 2	Comments
Default: $N = 40$, $\Delta t = \frac{\pi}{2000}$, $L_1 = L_2 = 4$, $W_0 = 3.2$	4.1307×10^{-4}	0.006547	
$N = 40$, $\Delta t = \frac{\pi}{500}$, $L_1 = L_2 = 4$, $W_0 = 3.2$	7.36253×10^{-4}	0.0117223	
$N = 40$, $\Delta t = \frac{\pi}{1000}$, $L_1 = L_2 = 4$, $W_0 = 3.2$	9.17225×10^{-4}	0.01459	
$N = 20$, $\Delta t = \frac{\pi}{2000}$, $L_1 = L_2 = 4$, $W_0 = 3.2$	0.00431	0.06928	
$N = 80$, $\Delta t = \frac{\pi}{2000}$, $L_1 = L_2 = 4$, $W_0 = 3.2$	6.4155×10^{-4}	0.01010	
$N = 160$, $\Delta t = \frac{\pi}{2000}$, $L_1 = L_2 = 4$, $W_0 = 3.2$	8.8087×10^{-4}	0.01383	
$N = 40$, $\Delta t = \frac{\pi}{2000}$, $L_1 = L_2 = 2$, $W_0 = 3.2$	0.13214	0.529303	
$N = 40$, $\Delta t = \frac{\pi}{2000}$, $L_1 = L_2 = 4$, $W_0 = 0.32$	0.1315411	0.6593023	Loss of height of the peak, increase of the probability outside the peak
$N = 40$, $\Delta t = \frac{\pi}{2000}$, $L_1 = L_2 = 4$, $W_0 = 0.032$	0.6598393	0.998853	Disappearance of the peak, density equal everywhere

2.3. Comparison with known 1 DOF systems

Following [12], we study this dynamical system:

$$\begin{cases} \dot{x} = y, \\ \dot{y} = -dy + x - x^3 + a\cos(\tau), \\ \dot{\tau} = 1. \end{cases} \tag{6}$$

The numerical values of the parameters are set: $d = 0.15$, $a = 0.3$, $W_0 = 0.01$, $N = 200$, $L_1 = 4$, $L_2 = 4$, $\Delta t = 0.2\pi$. Results of [12] are found again. By representing the Poincaré section, the two equilibrium points at $(x = \pm 1, y = 0)$ and the strange attractor can be seen (Fig. 3).

We study the parametric system of [16]:

$$\ddot{u} + \delta\dot{u} + \left(w_0^2 + \gamma\cos(wt)\right)u + \alpha u^2 + \beta u^3 = f(t), \tag{7}$$

$f(t)$ is a white noise of diffusion coefficient W_0.

For the numerical simulation, we choose the parameters of [16, p. 116], $\delta = 0.9$, $\gamma = 0.9$, $w_0 = 1$, $w = 1.895$, $\alpha = 1$, $\beta = 1$. If the initial condition chosen is a dirac located in the zone of attraction of the limit cycle of period $\frac{4\pi}{w}$, the Poincaré section is just a peak (see Fig. 4) located upon the fixed point corresponding to the periodic solution.

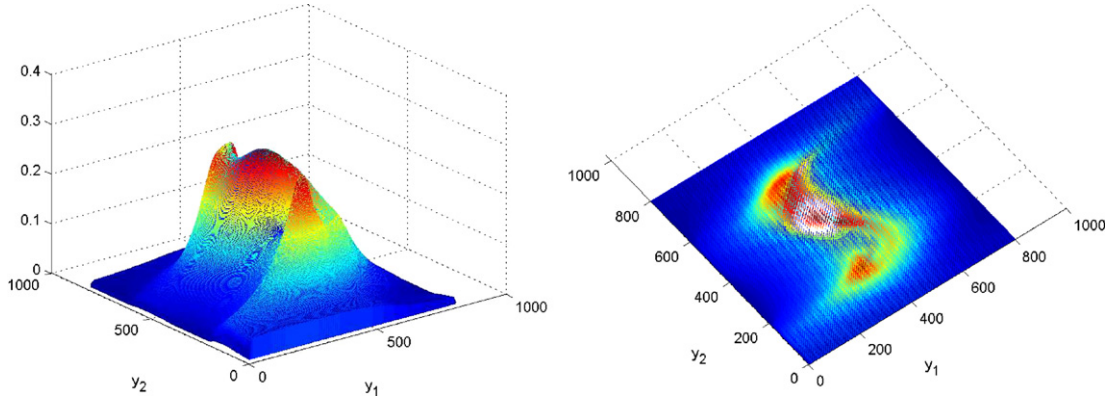

Fig. 3. Poincaré section of the Fokker–Planck probability density for the Duffing-like oscillator (6). Here $t = 90T$, where T is the period of the forcing.

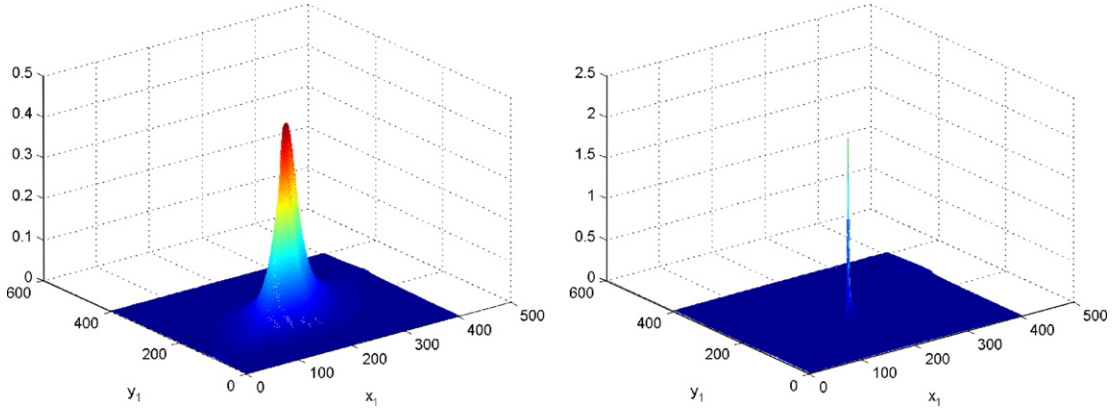

Fig. 4. Poincaré section of the system (7), with $\delta = 0.9$, $\gamma = 0.9$, $w_0 = 1$, $w = 1.895$, $\alpha = 1$, $\beta = 1$ and an initial condition located in the zone of attraction of the limit cycle of period $\frac{4\pi}{w}$. This section is given for $t = T$ (on the left) and $t = 40T$ (on the right).

To observe the other zones of attraction (those of the attractors with two or four strips), it is necessary to choose a convenient initial condition (see Figs. 5). Our results are coherent with complicated deterministic ones ([16]): the probability density plotted via Poincaré section of period $\frac{2\pi}{w}$ of Fig. 5 is spread upon attarctors.

2.4. Study of a quasi non-smooth system

The Fokker–Planck equation is difficult to obtain for non-smooth systems. We do not know mathematical results leading to a correct equation with additional boundary conditions corresponding to "obstacles" created by the associated "free boundary" problem: e.g. for impact problems, the displacement can be bounded, so the space variables in the Fokker–Palnck equation have a boundary. But in a purely non-smooth system, one has to add boundary conditions to solve the Fokker–Planck equation (see Fig. 6).

That is why we study the following quasi non-smooth system:

$$m\ddot{x} + a\dot{x} + kx + \alpha\sigma(\dot{x}) = r\sin(wt) + f(t), \tag{8}$$

where:

- $f(t)$ is a white noise whose diffusion coefficient is $\frac{W_0}{2}$.
- $\tilde{\sigma}(x)$ is the following function:

$$\tilde{\sigma}(x) = \begin{cases} -1 & \text{if } x < -\Delta y_1, \\ \frac{x}{\Delta y_1} & \text{if } x \in [-\Delta y_1, \Delta y_1], \\ 1 & \text{if } x > \Delta y_1. \end{cases}$$

The probabilistic results are similar to the deterministic ones, seen for example in [13]: for small times, the phase portrait has the shape of the line segment $\left[-\frac{\alpha}{k}, \frac{\alpha}{k}\right]$. After that, it looses its shape and rotate of quite 90°. Its form is that of an S, whose ends go on curving until looking like a snail.

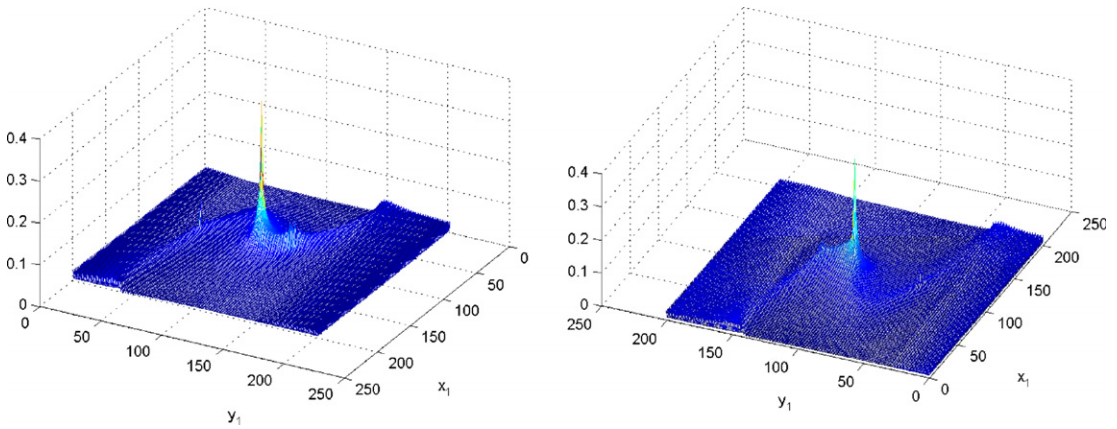

Fig. 5. Poincaré section of the system (7), with $\delta = 0.9$, $\gamma = 0.9$, $w_0 = 1$, $w = 1.895$, $\alpha = 1$, $\beta = 1$ and an initial condition located in the zone of attraction of the strange attractor with two strips.

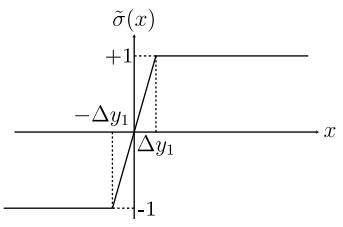

Fig. 6. Graph of the function as it is used in the simulation.

So with an amplitude of the sollicitation small, the evolution of the Fokker–Planck probability density function is the same: first, it has the shape of a line segment until a limit time (quite 0.3π here), then it bends. In the end, it winds around itself until having the shape of a snail (or a rose). For long times, this spiral spreads more and more. This behavior can be summed up by Fig. 7.

For long times, the ends of the S bends until having the shape of a snail Figs. 8 and 9, in agreement with deterministic mechanism.

3. Computation for 2 DOF systems

The term ''energy pumping'' means the transfer of energy from one mean structure to an auxiliary secondary one [7,8,28,5,25]. Here the mean structure is linear, whereas the other one is a non-linear, Duffing-like oscillator. We consider the following system:

$$\begin{cases} M\ddot{x} + \lambda_1\dot{x} + k_1 x + \gamma(x-y) = f_1(t), \\ m\ddot{y} + \lambda_s\dot{y} + Cy^3 + \gamma(y-x) = f_2(t), \end{cases} \tag{9}$$

with these initial conditions:

$$\begin{cases} x(0) = y(0) = \dot{y}(0) = 0, \\ \dot{x}(0) = \sqrt{2h} \end{cases} \tag{10}$$

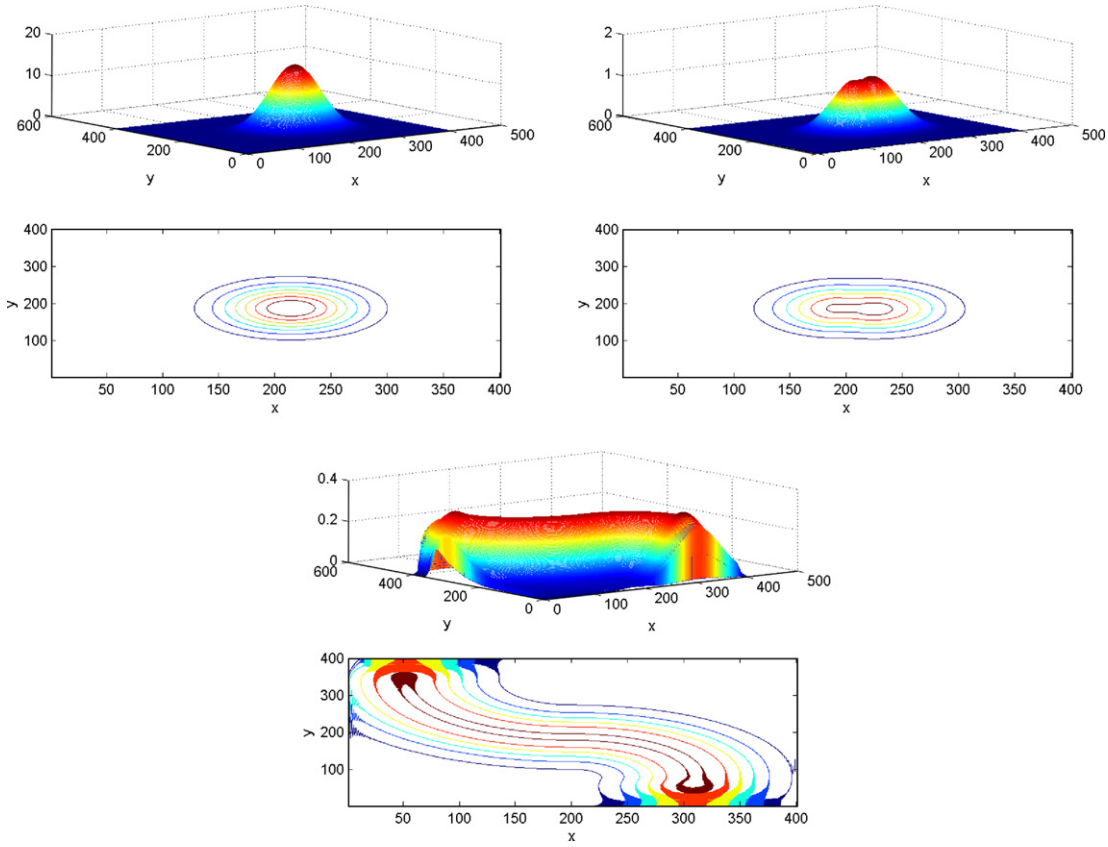

Fig. 7. Fokker–Planck probability density function of the dynamical system described by the Eq. (8) with $m = 1$, $a = 0.03$, $k = 1.0$, $\alpha = 1.0$, $r = 0.1$, $w = 0.9$. For this computation, we set the time-step $\Delta t = 0.001\pi$, the domain of study $[-1.5, 1.5] \times [-1.5, 1.5]$, the number of nodes in the mesh per direction is $N = 200$, the diffusion coefficient of the white noise is $W_0 = 0.001$. The initial condition is a gaussian centered in (0.1, 0.1). The times that are represented here are $t = 0$, $t = 30\Delta t$ and $t = 530\Delta t$. Thus we observe that the density function, that initially is a gaussian, takes the shape of a line segment from $-\frac{\alpha}{k}$ to $+\frac{\alpha}{k}$, which curves rapidly.

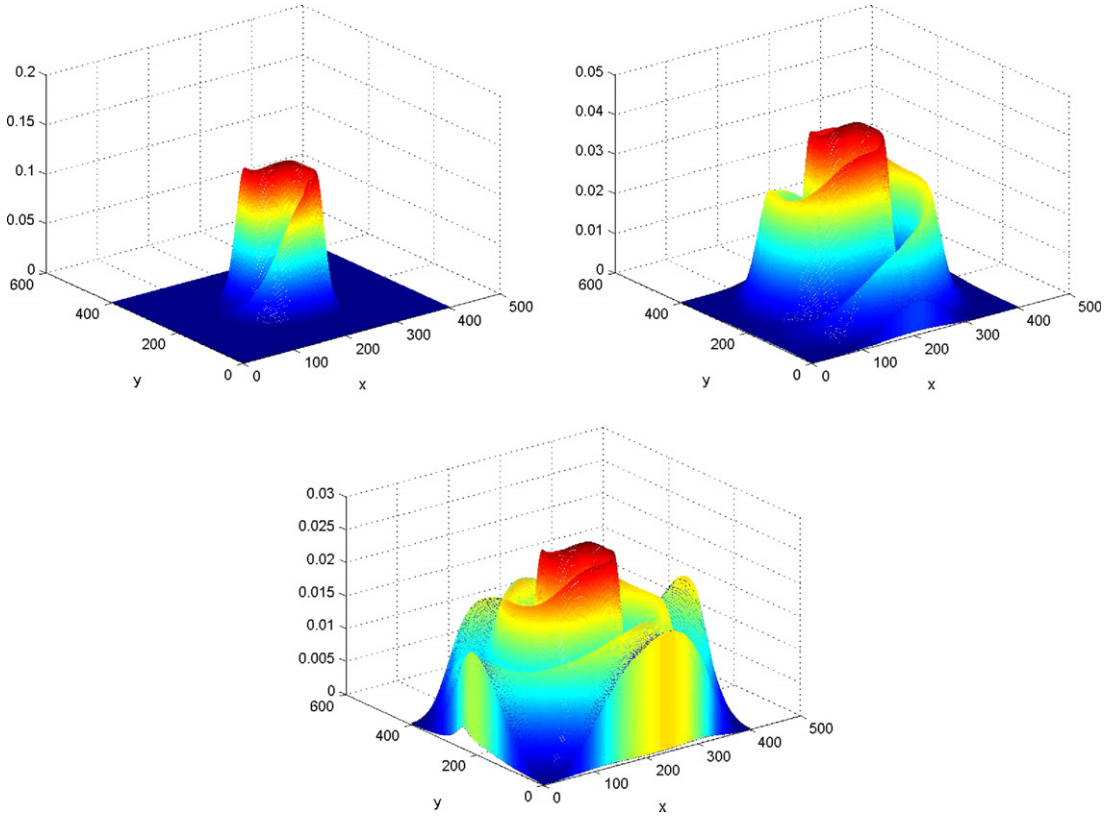

Fig. 8. Fokker–Planck probability density function of the same dynamical system as in graph (7). The times that are pictured are $10 \times 0.01\pi$, $20 \times 0.01\pi$ and $30 \times 0.01\pi$. So for important observation times, the line segment bends at its ends until having the shape of an"S". After that, it winds around itself until resembling a snail. But this phenomenon does not stop, it means that this density function goes on winding around, spreading more and more in space. So the domain study should be more and more vast as time increases.

and $f_1(t)$ and $f_2(t)$ are two white non-correlated noises whose diffusion coefficients are respectively W_{01} and W_{02}, so

$$\begin{cases} \langle f_1(t)\rangle = 0, \\ \langle f_2(t)\rangle = 0, \\ \forall (i,j) \in \{1,2\}^2, \quad \langle f_i(t_k)\cdot f_j(t_l)\rangle = \frac{W_{0i}}{2}\delta_{ij}\delta(t_k - t_l). \end{cases} \tag{11}$$

In the deterministic case ($f_1(t)=f_2(t)=0$), this energy pumping can be noticed through the positions of the two oscillators along time or the variation of their energy (see Fig. 10):

The Fokker–Planck equation for the system (9) is

$$\begin{aligned} \frac{\partial p}{\partial t} = & -y_2\frac{\partial p}{\partial y_1} + \frac{\partial}{\partial y_2}[(\lambda_1 y_2 + k_1 y_1 + \gamma(y_1 - y_3))p] + \frac{W_{01}}{4}\frac{\partial^2 p}{\partial y_2^2} - y_4\frac{\partial p}{\partial y_3} \\ & + \frac{\partial}{\partial y_4}[(\lambda_s y_4 + C y_3^3 + \gamma(y_3 - y_1))p] + \frac{W_{02}}{4}\frac{\partial^2 p}{\partial y_4^2}. \end{aligned} \tag{12}$$

We split this equation in six parts:

$$\frac{\partial p}{\partial t} = \mathscr{L}_1 p + \mathscr{L}_2 p + \mathscr{L}_3 p + \mathscr{L}_4 p + \mathscr{L}_5 p + \mathscr{L}_6 p, \tag{13}$$

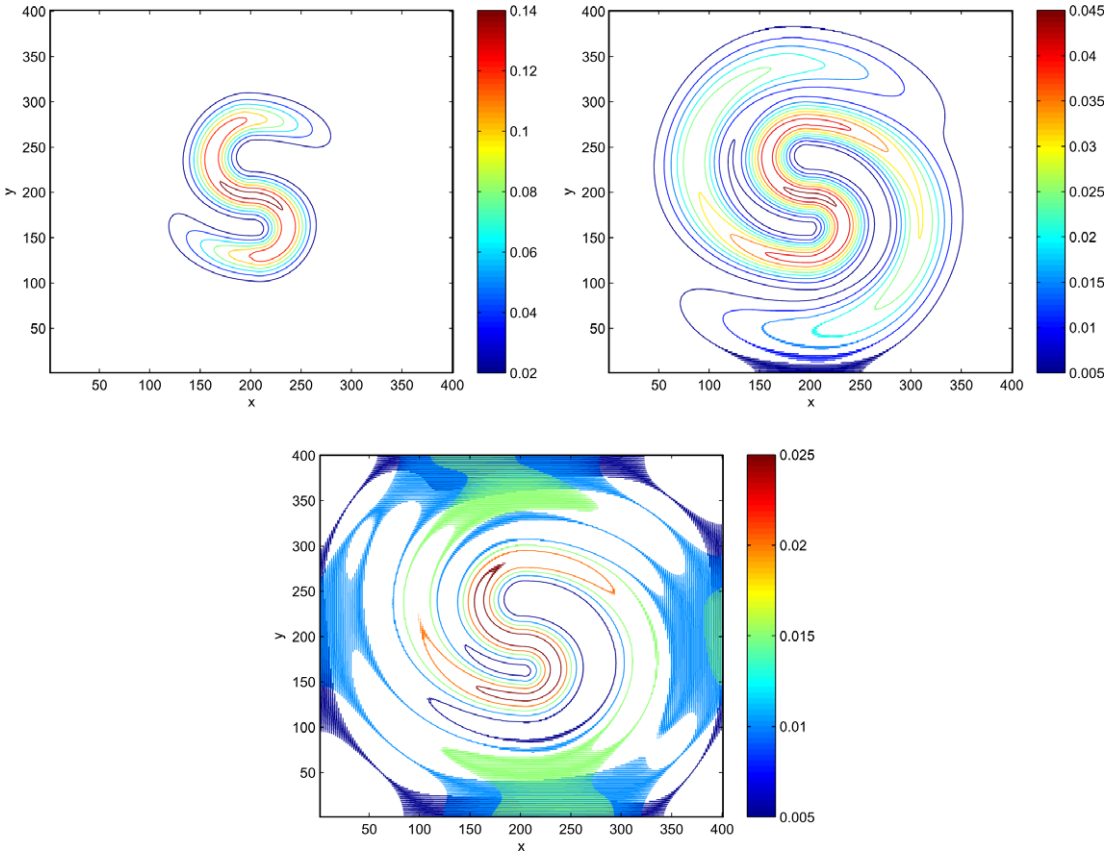

Fig. 9. Contours of the Fokker–Planck probability density function of picture 7. Chronologically the times are $10 \times 0.01\pi$, $20 \times 0.01\pi$ and $30 \times 0.01\pi$ (the sames as before, on Fig. 7).

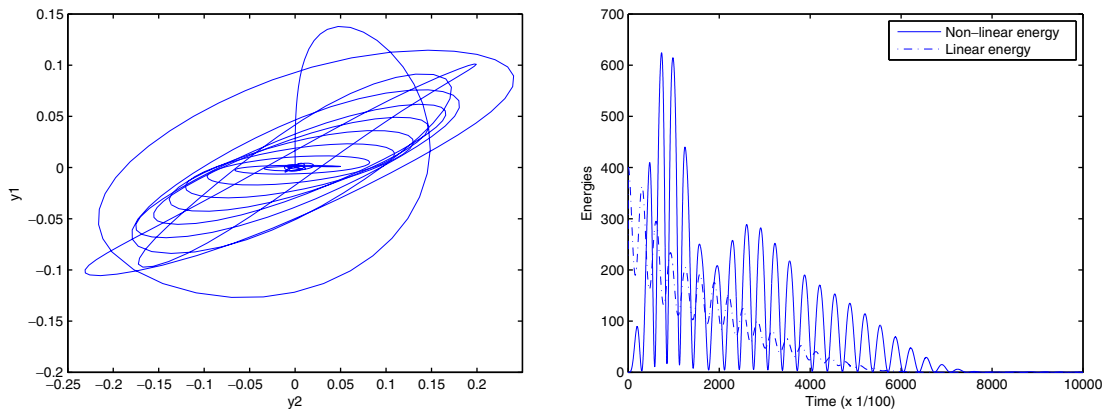

(a) Position of oscillator 2 versus position of oscillator 1.

(b) Energy of the two oscillators along time.

Fig. 10. Existence of energy pumping in system (9) with: $M = 1$, $\lambda_1 = 0.01$, $k_1 = 1$, $\gamma = 0.04$, $m = 0.05$, $\lambda_s = 0.01$, $C = 1$, $h = 0.1$ ([8]). At $t = 0$, only oscillator 1 is in motion (line quite vertical). Then the range of the oscillations of oscillator 1 increases until reaching a maximum (about 0.12), the oscillator 2 begins to oscillate. Energy is transferred, the oscillations y_2 are more and more important (curves more and more slopped). After that, the oscillator 2 is the only one to oscillate until reaching the complete rest. So when the linear energy reaches a threshold, the non-linear energy increases. After that, both decrease until being null.

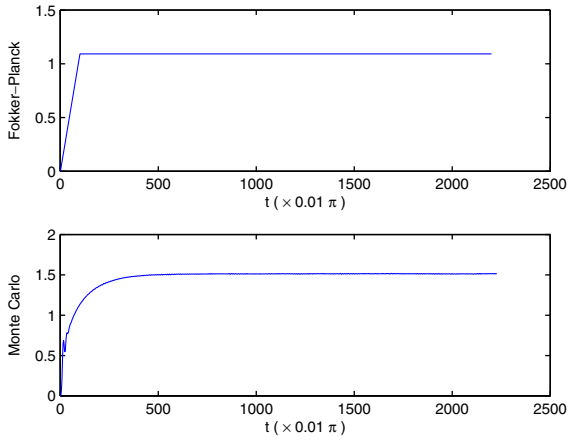

Fig. 11. Second moment of the position of the non-linear oscillator, of the system of Eq. (9), without sollicitation, $W_{01} = W_{02} = 40$ and $\Delta t = 0.01\pi$.

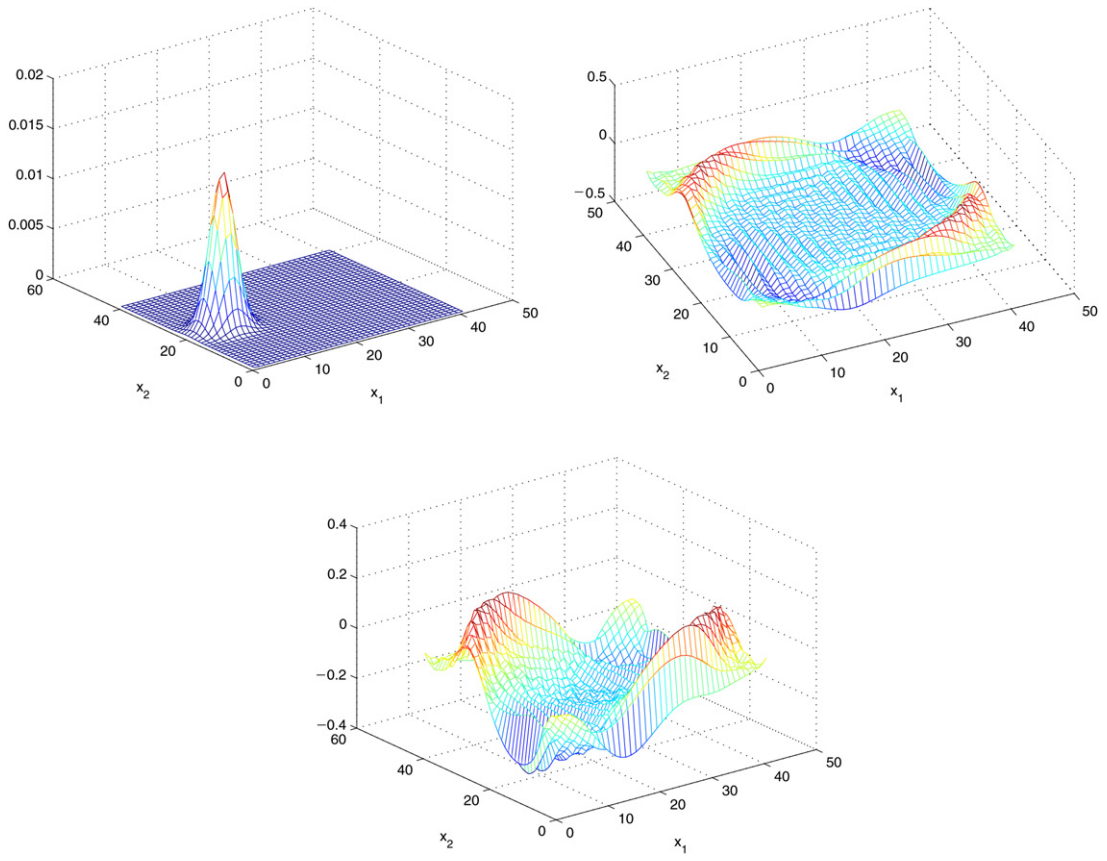

Fig. 12. Fokker–Planck probability density function of the first oscillator of Eq. (9) (the linear one) with parameters of Eq. (14). The times that are drawn here are $t = 0$, $t = 1000\Delta t$ and $t = 5900\Delta t$ (on the second line), with $\Delta t = 0.001\pi$. Initially, this oscillator is not at rest. But rapidly, its motion stops before spreading upon the track of the non-normal mode.

with $\mathscr{L}_1 = -y_2 \frac{\partial}{\partial y_1}$, $\mathscr{L}_2 = \frac{\partial}{\partial y_2}[\lambda_1 y_2 + k_1 y_1 + \gamma(y_1 - y_3)]$, $\mathscr{L}_3 = \frac{W_{01}}{2}\frac{\partial^2}{\partial y_2^2}$, $\mathscr{L}_4 = -y_4 \frac{\partial}{\partial y_3}$, $\mathscr{L}_5 = \frac{\partial}{\partial y_4}[\lambda_s y_4 + C y_3^3 + \gamma(y_3 - y_1)]$, $\mathscr{L}_6 = \frac{W_{02}}{2}\frac{\partial^2}{\partial y_4^2}$. To simulate this Fokker–Planck equation, we use the following numerical values of the parameters (according to [7]):

$$\begin{cases} k_1 = 4000\ \mathrm{N\ m^{-1}}, \\ \lambda_1 = 100\ \mathrm{N\ s\ m^{-1}}, \\ M = 4000\ \mathrm{Kg}, \\ \gamma = 1000\ \mathrm{N\ m^{-1}}, \\ m = 4000\ \mathrm{Kg}, \\ \lambda_s = 300\ \mathrm{N\ s\ m^{-1}}, \\ C = 600\ \mathrm{N\ m^{-3}}. \end{cases} \tag{14}$$

Moreover, we choose the following parameters of the simulation: $W_0 = 10$, $\Delta t = 0.01\pi$, $N = 20$, $L_1 = L_2 = L_3 = L_4 = 6.0$.

In order to check the accuracy of the solution obtained through numerical integration of the Fokker–Planck equation, we perform Monte Carlo simulations using the fact that the system of dynamical Eq. (9) can also be written as a system of two stochastic differential equations. We choose Itô's stochastic calculus, so:

$$\begin{cases} \mathrm{d}X_1(t) = X_2(t)\mathrm{d}t, \\ \mathrm{d}X_2(t) = \left[-\frac{\lambda_1}{M}X_2(t) - \frac{k_1}{M}X_1(t) - \frac{\gamma}{M}(X_1(t) - X_3(t))\right]\mathrm{d}t + \mathrm{d}W_1(t), \\ \mathrm{d}X_3(t) = X_4(t)\mathrm{d}t, \\ \mathrm{d}X_4(t) = \left[-\frac{\lambda_s}{m}X_4(t) - \frac{c}{m}X_3^3(t) - \frac{\gamma}{m}(X_3(t) - X_1(t))\right]\mathrm{d}t + \mathrm{d}W_2(t), \end{cases} \tag{15}$$

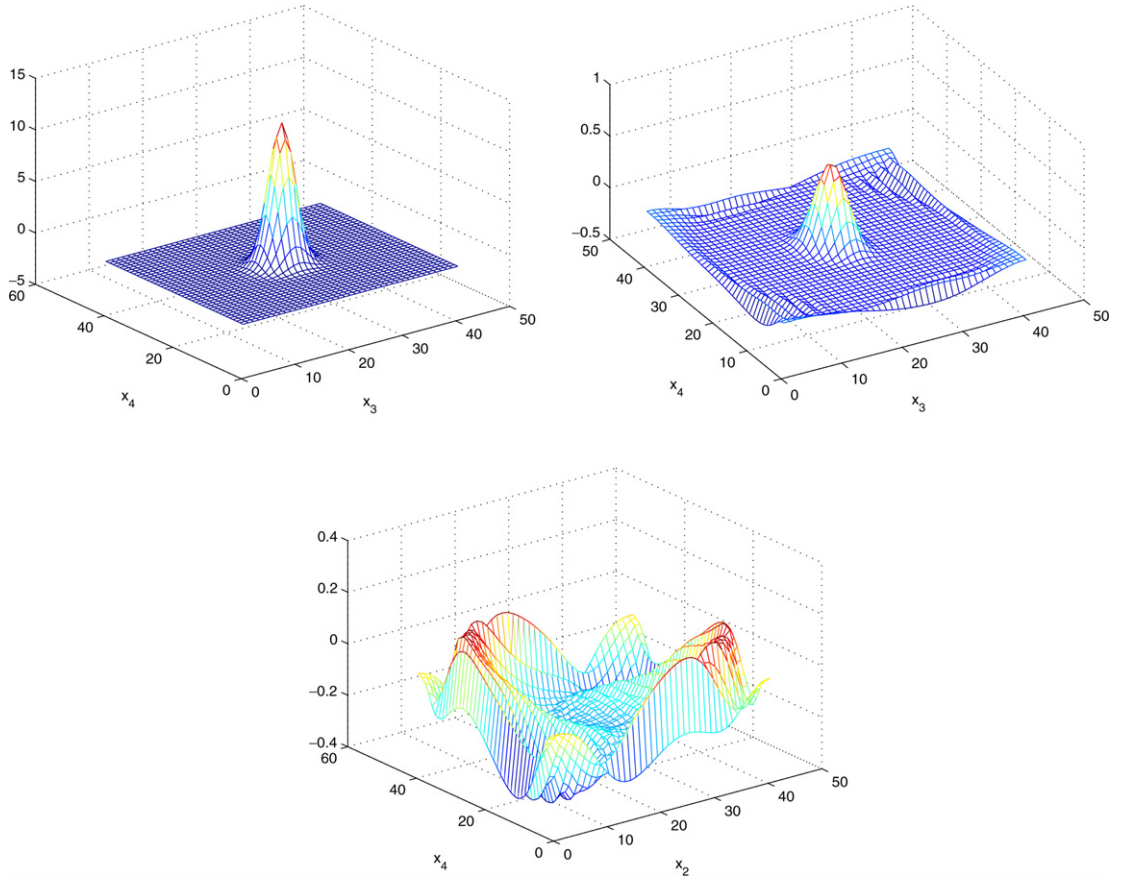

Fig. 13. Fokker–Planck probability density function of the system of Eq. (9) with parameters of Eq. (14). The times that are drawn here are $t = 0$, $t = 200\Delta t$ and $t = 5900\Delta t$ (on the second line), with $\Delta t = 0.001\pi$. This non-linear oscillator is initially at rest. Then rapidly, it moves and forms the non-normal mode.

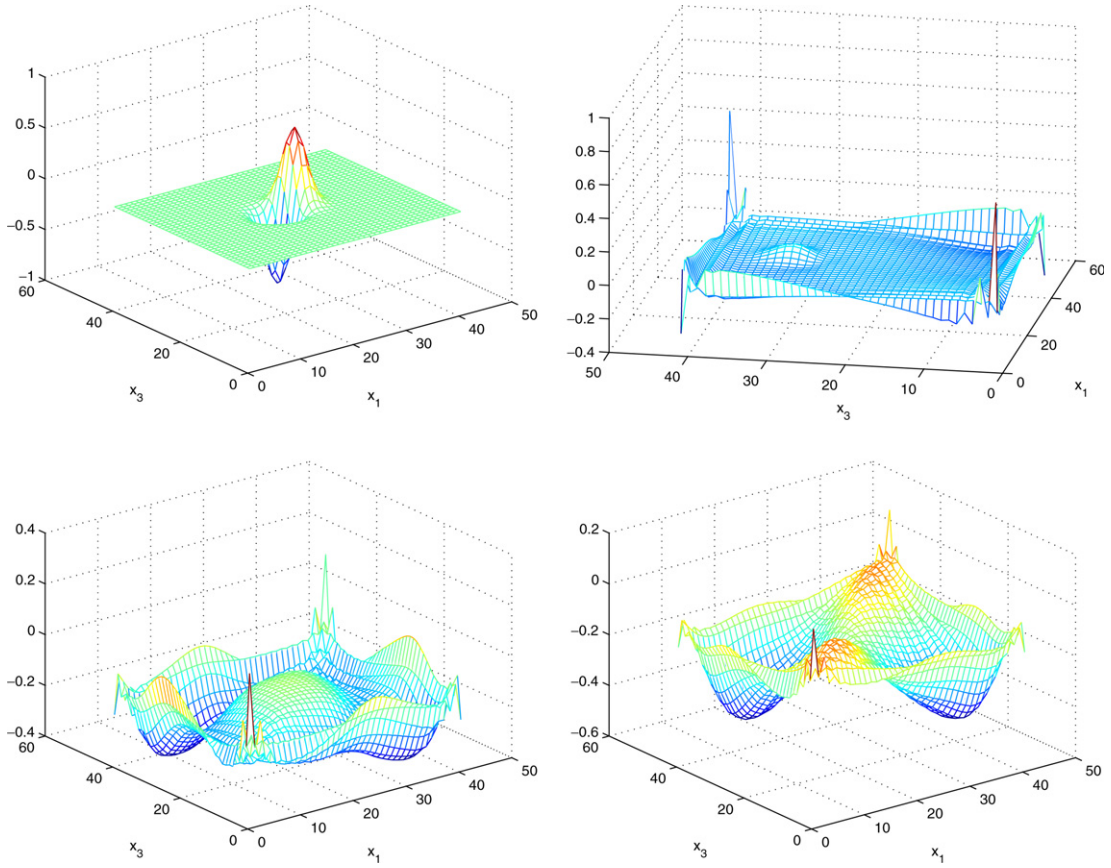

Fig. 14. Fokker–Planck probability density function of the positions x and y of the system of Eq. (9) with parameters of Eq. (14). The times that are pictured are $t = 0$ $t = 200\Delta t$, $t = 500\Delta t$ and $t = 5900\Delta t$, with $\Delta t = 0.001\pi$.

with $\begin{Bmatrix} X_1(0) = X_{10} \\ X_2(0) = X_{20} \\ X_3(0) = X_{30} \\ X_4(0) = X_{40} \end{Bmatrix}$, $0 \leqslant t \leqslant T$ [9,10]. By setting $X(t) = \begin{Bmatrix} X_1(t) \\ X_2(t) \\ X_3(t) \\ X_4(t) \end{Bmatrix}$,

$f(X) = \begin{Bmatrix} X_2(t) \\ -\frac{\lambda_1}{M}X_2(t) - \frac{k_1}{M}X_1(t) - \frac{\gamma}{M}(X_1(t) - X_3(t)) \\ X_4(t) \\ -\frac{\lambda_s}{m}X_4(t) - \frac{c}{m}X_3^3(t) - \frac{\gamma}{m}(X_3(t) - X_1(t)) \end{Bmatrix}$, $g(X) = \begin{Bmatrix} 0 \\ 1 \\ 0 \\ 1 \end{Bmatrix}$ and $W = \begin{Bmatrix} 0 \\ W_1(t) \\ 0 \\ W_2(t) \end{Bmatrix}$, we can write

Eq. (15) in the form:

$$\mathrm{d}X(t) = f(X(t))\mathrm{d}t + g(X(t)) \cdot \mathrm{d}W(t), \quad X(0) = X_0, \ 0 \leqslant t \leqslant T. \tag{16}$$

The functions $f(x)$ et $g(x)$ are continuous (and in particular, right-continuous with a limit to the left and lipschiz-continuous), so we can claim [2–4,20] the existence and unicity of the solution of 16.

While comparing the moments of the motion calculated through Monte Carlo simulation (simulation of the white noise) and those assessed via the Fokker–Planck probability density function, we observe that they are similar but not equal (see Fig. 11). It is difficult to know which one of these methods is the most false. Indeed, the Monte Carlo simulation needs many draws and much time before converging.

The issue is that the density function is given by arrays belonging to $\mathbb{R}^4$. So to represent the phenomenon of energy pumping, we may calculate marginal probability densities depending just on two variables. Here we

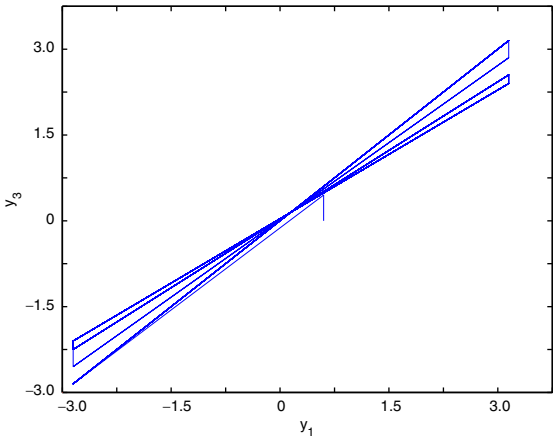

Fig. 15. Maximum in $x(=y_1)$ and $y(=y_3)$ of the Fokker–Planck probability density function along time. This probabilistic result is quite the same as the deterministic one (Fig. 10). The only difference is that in this case, the phenomenon of energy pumping is not finished. This is probably due to the white noise which is always present.

choose to focus on the marginal density of the first oscillator, that of the second one and the marginal density of the two positions.

The Fokker–Planck probability density function of the linear oscillator first presents the gaussian initial condition centered on $(0, \sqrt{2h})$. Then it flattens before taking the shape of the non-normal mode [27], as can be seen in Fig. 12.

Now, if we study the probability density function for the second oscillator of the system following equation (9). We first see the initial condition which is gaussian and located in $(0,0)$. Then the peak disappears and the probability density takes the shape of the non-normal mode Fig. 13.

Finally, the Fokker–Planck probability density function of the positions of both oscillators also proves the phenomenon of energy pumping Fig. 14.

Thus, in 2DOF systems, the deterministic aspects of energy pumping can be meet in this probabilistic study. So, the non-normal modes can be seen if we represent the position of the maximum of probability along time Fig. 15.

These simulations have been made with 41 nodes of the mesh in every direction. In these calculations which work on matrices belonging to $\mathbb{R}^4$, it is possible to decrease the step in space until having 104 nodes of the mesh per direction. But the time of calculation incresases then exponentially.

Moreover, the domain of study chosen here is $L_1 = L_2 = L_3 = L_4 = 6$. Indeed, it seems sufficiently large to take into account of all the dynamics of the system. It could be determined by a deterministic study.

4. Conclusion

In this article, after having written the Fokker–Planck equation in the general case, we proposed a way to resolve it by means of the finite difference method. Then we proved this calculation to be correct and accurate for one DOF systems by comparing it with the analytical solution of a specific case. Finally we studied the motion of some systems: a Duffing-like oscillator whose equilibrium points and strange attractors have so been revealed, a system with Coulomb friction and a two-degree-of-freedom system taking place to energy pumping.

Thus we claim that this method is acceptable for investigating non-linear dynamics of one DOF systems in real noisy environment. For two DOF, it can be used in order to obtain qualitative information. Indeed, the exact error cannot be calculated and the simulation is time-consuming and limited (for an ordinary computer). But it may be quite efficient way to test robustness of the energy pumping phenomenon under white noise that may stand for a random forcing (e.g. earthquake) or the intrinsic parameters of the systems that may not be known precisely (e.g. for a building).

Acknowledgement

This work has been partially supported by the contract ANR BLAN07-1_188624 (ADYNO).

References

[1] Dessombz O, Thouverez F, Laîne J-P, Jézéquel L. Analysis of mechanical systems using interval computations applied to finite element methods. J Sound Vib 2001;239(5):949–68.
[2] Doléans-Dade C. Existence and unicity of solutions of stochastic differential equations. Z für Wahrscheinlichkeitstheorie und Verw Gebiete 1976;36(2):93–102.
[3] Doléans-Dade C, Meyer P-A. Equations différentielles stochastiques. In: Irma, editor. Séminaire de probabilités, vol. 11. Strasbourg: Springer-Verlag; 1977. p. 376–82.
[4] Doss H, Lenglart E. Sur l'existence, l'unicité et le comportement asymptotique des solutions d'équations différentielles stochastiques. Annales de l'I.H.P. section B 1978;14(2):189–214.
[5] Gendelman OV, Lamarque CH. Dynamics of linear oscillator coupled to strongly nonlinear attachment with multiple states of equilibrium. Chaos, Solitons & Fractals 2005;24(2):501–9.
[6] Ghanem RG, Spanos PD. Stochastic finite elements: A spectral approach. Springer; 1991.
[7] Gourdon E, Lamarque CH. Energy pumping for a larger span of energy. J Sound Vib 2005;285(3):711–20.
[8] Gourdon E, Lamarque CH. Energy pumping with various nonlinear structures: Numerical evidences. Nonlinear Dyn 2005;40(3):281–307.
[9] Higham DJ. An algorithmic introduction to numerical simulation of stochastic differential equations. Soc Ind Appl Math 2001;43(3):525–46.
[10] Kloeden PE, Platen E. Numerical solution of stochastic differential equations. 3rd ed. New York: Springer; 1992.
[11] Kourakis I, Grecos A. Plasma diffusion and relaxation in a magnetic field. Communications in nonlinear science and numerical simulation chaotic transport and compexity in classical and quantum dynamics 2003;8(3–4):547–51.
[12] Kunert A, Pfeiffer F. Description of chaotic motion by an invariant probability. Nonlinear Dyn 1991;2(4):291–304.
[13] Lamarque C-H, Bastien J. Numerical study of a forced pendulum with friction. Nonlinear Dyn 2000;23(4):335–52.
[14] Lohmiller W, Slotine J-JE. On contraction analysis for non-linear systems. Automatica 1998;34(6):683–96.
[15] Mace BR, Worden K, Manson G. Uncertainty in structural dynamics. J Sound Vib 2005;288(3):423–9.
[16] Malasoma J-M. Dynamique complexe d'un système à attracteurs multiples. PhD thesis, Ecole Centrale de Lyon; 1994.
[17] Neelakanta PS, Abusalah ST, De Groff DF, Park JC. Fuzzy nonlinear activity and dynamics of fuzzy uncertainty in the neural complex. Neurocomputing 1998;20(1–3):123–53.
[18] Oseledec VI. A multiplicative ergodic theorem: Lyapunov characteristic numbers for dynamical systems. Trans Moscow Math Soc 1968;19:197–231.
[19] Press WH, Flannery BP, Teukolsky SA, Vetterling WT. Numerical recipes in C: the art of scientific computing. Cambridge: Cambridge University Press; 1992.
[20] Protter PhE. On the existence, uniqueness, convergence and explosions of solutions of systems of stochastic integral equations. Ann Prob 1977;5(2):243–61.
[21] Risken H. The Fokker–Planck equation. Methods of solution and applications, volume Springer Series in Synergetics. 2nd ed. Berlin: Springer-Verlag; 1989.
[22] Schueller GI. A state-of-the-art report on computational stochastic mechanics. Prob Eng Mech 1997;12(4):197–321.
[23] Slotine JJE, Lohmiller W. Modularity, evolution, and the binding problem: a view from stability theory. Neural Networks 2001;14(2):137–45.
[24] Soize C. Random matrix theory for modeling uncertainties in computational mechanics. Comput Meth Appl Mech Eng Special Issue on Computational Methods in Stochastic Mechanics and Reliability Analysis 2005;194(12–16):1333–66.
[25] Tsakirtzis S, Kerschen G, Panagopoulos PN, Vakakis AF. Multi-frequency nonlinear energy transfer from linear oscillators to MDOF essentially nonlinear attachments. J Sound Vib 2005;285(1–2):483–90.
[26] Gazanfer Unal, Jian-Qiao Sun. New exact solutions to the Fokker–Planck–Kolmogorov equation. Commun Nonlinear Sci Numer Simul, in press.
[27] Vakakis AF. Non-linear normal modes (NNMS) and their applications in vibration theory: an overview. Mech Syst Signal Process 1997;11(1):3–22.
[28] Vakakis AF, Manevitch LI, Gendelman O, Bergman L. Dynamics of linear discrete systems connected to local, essentially non-linear attachments. J Sound Vib 2003;264(3):559–77.
[29] Zorzano MP, Mais H, Vazquez L. Numerical solution for Fokker–Planck equations in accelerators. Physica D: Nonlinear Phenomena Proceedings of the Conference on Fluctuations, Nonlinearity and Disorder in Condensed Matter and Biological Physics 1998;113(2–4):379–81.
[30] Zorzano M-P, Mancho AM, Vazquez L. Numerical integration of the discrete-ordinate radiative transfer equation in strongly non-homogeneous media. Appl Math Comput 2005;164(1):263–74.
[31] Zorzano MP, Mais H, Vazquez L. Numerical solution of two dimensional Fokker–Planck equations. Appl Math Comput 1999;98(2–3):109–17.